Probabilistic Approach-based Wide-Area Damping Controller for Small-Signal Stability Enhancement of Wind-Thermal Power Systems

C. A. Juárez, *Graduate Student Member, IEEE*, J. L. Rueda, *Member, IEEE*,
I. Erlich, *Senior Member, IEEE*, and D. G. Colomé

***Abstract*—Based on wide area measurements obtained by phasor measurement units and probabilistic eigenanalysis, this paper presents an approach to the design of a wide-area supplementary damping controller (WASDC) in order to improve the damping of inter-area oscillatory modes in wind-thermal power systems. Novel probabilistic indexes of controllability and observability are proposed to tackle the selection of proper wide-area input signals and the placement of the WASDC. Parameters of the controller are determined by solving an optimization problem that accounts for small-signal stability performance requirements. Numerical results obtained using a benchmark weak interconnected power system are used to survey the possible impact of wind power on system small-signal stability performance, especially in terms of mode controllability and observability, as well as to demonstrate the effectiveness of the proposed controller.**

***Index Terms*—Small-Signal Stability, Inter-area Oscillations, Wide-area measurements, Eigenanalysis, Probabilistic Indexes, Controllability, Observability, Wide-area Control.**

I. Introduction

THE evolution of the electric power industry toward increasingly complex interconnected networks, which operate under deregulated electricity markets with open access of transmission systems and greater and greater incorporation of significant amounts of renewable generating systems with intrinsic variable behavior, has significantly affected power system management. As of this writing, many power systems worldwide are often forced to operate closer to their security limits due to several factors, such as greater competition between agents, market pressures, reduced generation reserve margins, lack of transmission expansion, and bulk power exchanges over long distances, to name a few. These factors increase the possible sources of system disturbances, thus increasing system vulnerability to small-signal stability problems as evidenced in recent literature [1]. Most of these problems usually manifest as poorly damped, sustained or growing inter-area oscillations, typically in the range of 0.1 to 2.0 Hz, which can potentially led to unstable system operation with major consequences including grid breakups and widespread blackouts [2]. Consequently, many technical and economic issues have arisen and the need for small-signal stability studies and measures to minimize the occurrence and impact of inter-area oscillations in the context of power system operation with changing charactetistics is drawing more attention from power system engineers.

Many utilities have established security requirements which should be satisfied in power system planning and operation in order to ensure well damped oscillations. Amongst these is the damping ratio threshold (i.e. a metric inversely related to the number of cycles for an oscillation to decay) [3]. Moreover, it is well known that due to due to the inherent limitations of power systems to damp out low frequency oscillations, power system controllers and some countermeasures play a vital role in enhancing system damping performance [2].

From power system operation perspective, much work has been directed towards the development of methods for improving system small-signal stability performance through operational strategies such as generation rescheduling methods [4] and coordination of transmission path transfers [5]. Other innovative methods suggest optimal power flow computation including small-signal stability constraints [6] and computational intelligence based optimal adjustment of power flows and bus voltages features [7].

Besides, considerable effort has gone into the research area of supplementary damping controllers. The traditional approach to damping control design in a power system is to add power system stabilizers (PSSs), which are mostly single-loop local controllers [8]. But this kind of control design cannot always prove to be effective in damping inter-area modes [8]. Local controllers lack global observability, mutual coordination and placement flexibility [9]-[10]. Nowadays, there are important efforts to improve supplementary damping control, monitoring and supervision in power systems, which are mainly related to the development of the wide-area measurement system technology (WAMS) [11].

WAMS involves distributed phasor measurements throughout the network by means phasor measurement units (PMUs). All phasors are synchronized using the same GPS (Global Positioning System) system time source (i.e. GPS-

This work was supported by the German Academic Exchange Service, the University Duisburg-Essen and by Universidad Nacional de San Juan.

C. A. Juárez and D: G. Colome are with Instituto de Energía Eléctrica, Universidad Nacional de San Juan, San Juan, 5400, Argentina (e-mail: cjuarez@iee.unsj.edu.ar, colome@iee.unsj.edu.ar).

J. L. Rueda and I. Erlich are with the Department of Electrical Power Systems, University Duisburg-Essen, Duisburg, 47057, Germany (e-mail: jose.rueda@uni-duisburg-essen.de, istvan.erlich@uni-due.de).

978-1-4577-1002-5/11/$26.00 ©2011 IEEE

synchronized phasors). PMUs are in general higher precision equipment as compared to typical SCADA systems [12]. One goal of WAMS is to provide critical information about the oscillatory behavior of power systems [13]. In this connection, a WASDC design approach based on probabilistic eigenanalysis is provided in this paper. For this purpose, the so-called concept of synthetic controllability and observability is firstly extended to the probabilistic context through a settled probabilistic eigenanalysis method in order to determine suitable controller location as well as to perform proper selection of the input signal of the controller. Also, the tuning of the controller through particle swarm optimization (PSO) is realized under constraints that accounts for small-signal stability performance requirements.

The outline of the paper is as follows: Section II gives some background information on state-space modeling of power systems. The proposed approach is described in Section III. Application of the proposed approach to a benchmark weak interconnected power system, showing the effectiveness of the WASDC and providing information on the impact of different wind power generation levels on system small-signal stability performance, is presented in Section IV. Section V concludes.

II. State-Space Modeling

A power system is a nonlinear system which can be described by the following set of nonlinear equations:

$$\dot{\mathbf{x}}_s = \mathbf{f}(\mathbf{x}_s, \mathbf{x}_a, \mathbf{u}), \quad \mathbf{x}_s \in \mathbf{R}^n \quad \mathbf{u} \in \mathbf{R}^p \tag{1}$$

$$0 = \mathbf{g}(\mathbf{x}_s, \mathbf{x}_a, \mathbf{u}), \quad \mathbf{x}_a \in \mathbf{R}^m \tag{2}$$

$$\mathbf{y} = \mathbf{h}(\mathbf{x}_s, \mathbf{x}_a), \quad \mathbf{y} \in \mathbf{R}^q \tag{3}$$

where (1) models differential equations of dynamic devices, $\mathbf{x_s}$ represents state variables, $\mathbf{x_a}$ represents algebraic variables (e.g. magnitude and phase of node voltages), $\mathbf{u}$ represents input variables and $\mathbf{y}$ denotes output variables. Assuming that input control variables $\mathbf{u}$ do not directly affect the outputs, the linear representation of (1) around a system operating point, which is suitable to analyze small disturbances in the power system, is expressed as follows [2]:

$$\Delta\dot{\mathbf{x}}_s = \mathbf{A}_{11}\Delta\mathbf{x}_s + \mathbf{A}_{12}\Delta\mathbf{x}_a + \mathbf{B}_1\Delta\mathbf{u} \tag{4}$$

$$0 = \mathbf{A}_{21}\Delta\mathbf{x}_s + \mathbf{A}_{22}\Delta\mathbf{x}_a + \mathbf{B}_2\Delta\mathbf{u} \tag{5}$$

$$\Delta\mathbf{y} = \mathbf{C}_1\Delta\mathbf{x}_s + \mathbf{C}_2\Delta\mathbf{x}_a \tag{6}$$

Without algebraic variables the set of equations (4)-(6) can be reduced to the following form:

$$\Delta\dot{\mathbf{x}}_s = \mathbf{A}\Delta\mathbf{x}_s + \mathbf{B}\Delta\mathbf{u} \tag{7}$$

$$\Delta\mathbf{y} = \mathbf{C}\Delta\mathbf{x}_s \tag{8}$$

where,

$$\mathbf{A} = \mathbf{A}_{11} - \mathbf{A}_{12}\mathbf{A}_{22}^{-1}\mathbf{A}_{21} \tag{9}$$

$$\mathbf{B} = \mathbf{B}_1 - \mathbf{A}_{12}\mathbf{A}_{22}^{-1}\mathbf{B}_2 \tag{10}$$

$$\mathbf{C} = \mathbf{C}_1 - \mathbf{C}_2\mathbf{A}_{22}^{-1}\mathbf{A}_{21} \tag{11}$$

The small signal stability is given by the eigenvalues (i.e. λ_i, i=1…n) of state matrix $\boldsymbol{A}$ [8]. For any eigenvalue λ_i, there are the corresponding vectors: right eigenvector (ϕ_i), and left eigenvector (ψ_i). The right eigenvector gives the mode shape, which is the relative activity of state variables when a particular mode is excited. The magnitudes of the right eigenvector elements give the extents of the activities of the n state variables in the i-th mode, and the angles of the elements give phase displacements of the state variables with regard to the mode [2]. The left eigenvector is referring to the initial conditions, since it has a direct effect on the amplitude of a mode excited by a specific input [8]

III. Proposed Approach

A. Probabilistic eigenanalysis

The flowchart of the Monte Carlo based-probabilistic eigenanalysis is illustrated in Fig. 1 [14]. The procedure starts with the definition of the models required for power system dynamic analysis, the probabilistic models of system input variables (i.e. probability distribution functions of nodal loads and mean values of the coefficients defining piecewise quadratic cost functions of thermal generating units) and the requirements for small-signal stability performance (e.g. damping ratio threshold imposed on the system by the small-signal stability constraint in order to guarantee secure operation). Next, samples of nodal demands are generated according to their probability distribution function models. Based on a settled utility's operating policy to balance power (e.g. least-cost or merit-order economic dispatch), a set of generation variables corresponding to each set of sampled nodal demands is obtained (i.e. all components of the input nodal vector are obtained).

Each trial input vector defines an operating state which is determined by power flow calculation. Viable operating states that fulfill steady state voltage limits, thermal overloading of transmission elements, and maintain the generation units operating within their limits are then selected. Next, the system small-signal stability performance is evaluated via modal analysis for each viable operating state. Here, critical modes, their associated frequency, damping ratio ζ, right eigenvectors and left eigenvectors are calculated. An eigenvalue tracking procedure based on modal parameters is also applied at this stage to ensure proper storage of modal analysis information and to ensure proper statistical evaluation of computed critical mode parameters. Besides, sequential estimation of statistical relative error is applied in probabilistic eigenanalysis in order to ensure a high degree of confidence. Thereafter, the resulting mode frequency and damping statistics are defined in terms of their respective mean values and standard deviations. Also, the probabilistic index R_{Inst} is calculated to assess the instability risk due to negatively damped or lowly damped oscillatory modes (OMs). Based on a defined ζ threshold (e.g. $\zeta i > 5\%$), the R_{Inst} index is calculated accounting the cumulative probability distribution function (CPDF) associated to each critical mode ζ as follows

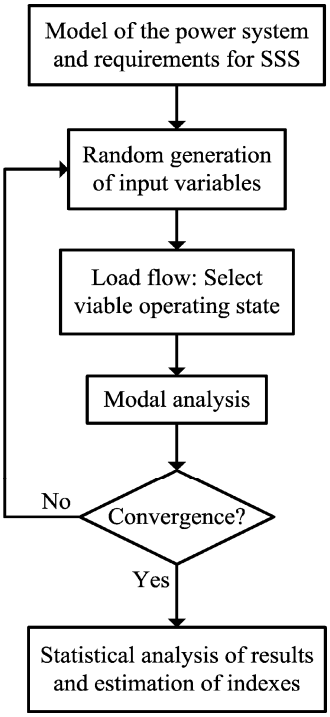

Fig. 1. Monte Carlo-based probabilistic eigenanalysis

$$R_{Inst}=\begin{cases}OM_{\zeta\text{-Neg}}=P(\zeta_i<0)\\ OM_{\zeta\text{-Poor}}=P(0\le\zeta_i<5\%)\ i=1,\cdots,M_C\\ OM_{\zeta\text{-Damp}}=P(\zeta_i\ge5\%)\end{cases} \quad (12)$$

where $OM_{\zeta\text{-Neg}}$ indicates the probability of instability due to negatively damped OM, $OM_{\zeta\text{-Poor}}$ indicates the probability associated to poorly damped OM, and $OM_{\zeta\text{-Damp}}$ indicates the probability associated to well damped OM. M_C is the number of critical modes, and P(.) denotes cumulative probability.

B. Probabilistic Observability and Controllability Indexes

Wide-area control is desirable for inter-area oscillation damping, since it mainly provides better observability and controllability measures, which would entail more effective influence on damping of this oscillation type [15]. Therefore, one goal of WADC design is to define proper placing observer and input signal.

In this paper, probabilistic indexes of controllability and observability are calculated based on the so-called method of geometric measures of controllability and observability (GMCO), which were introduced in [16], to determine the most effective stabilizing signals and suitable control locations. The GMCO method has proven to be more reliable than the residues approach as reported in [15]-[17]. The geometric measures of controllability gm_{ci} and observability gm_{oi} associated with the i-th mode are defined as follows [16]:

$$gm_{ci}(k)=\cos(\theta(\psi_i,b_k))=\frac{|\psi_i b_k|}{\|\psi_i\|\|b_k\|} \quad (13)$$

$$gm_{oi}(l)=\cos(\theta(c_l,\phi_i))=\frac{|c_l\phi_i|}{\|c_l\|\|\phi_i\|} \quad (14)$$

where b_k is the k-th column of the input matrix **B** (corresponding to the k-th input), c_l is the l-th row of the output matrix **C** (corresponding to the l-th output). |.| and ||.|| denotes modulus and Euclidean norm**,** respectively. $\theta(\psi_i, b_k)$ is the geometrical angle between the k-th input vector and the i-th left eigenvector, whereas $\theta(c_l,\phi_i)$ is the geometrical angle between the l-th output vector and the i-th right eigenvector.

These geometric measures of controllability and observability are calculated at each iteration of the Monte Carlo-based probabilistic eigenanalysis. Hence, their corresponding mean values and standard deviations define probabilistic measures of gm_{ci} and gm_{oi}, respectively, which form the basis for screening of the most suitable input of the controller and its location.

C. WASDC structure

The WASDC provides an extra stabilizing signal (V_{swadc}) as an additional input superimposed on the voltage control loop of the AVR (automatic voltage regulator) of a given generator. The key goal is to improve the damping of critical inter-area modes. Fig. 2 illustrates schematically the structure of the controller. Initially, all conventional synchronous generators belonging to the power system are potential candidates for controller location. The selection of controller location (i.e. generator) and feedback signal (i.e. PMU measurement), is given by highest mean values of controllability and observability indexes obtained through probabilistic analysis, respectively.

D. Tuning of the WASDC

The block diagram of the WASDC is depicted in Fig. 3. It comprises a gain block, a washout filter, and two lead-lag blocks. As noted in Fig. 2, the WASDC output is summed to the reference of the excitation system. The implementation the WASDC involves the transmission to power plants of remote signals acquired through PMU. Therefore, time delays must be also considered when tuning the controller.

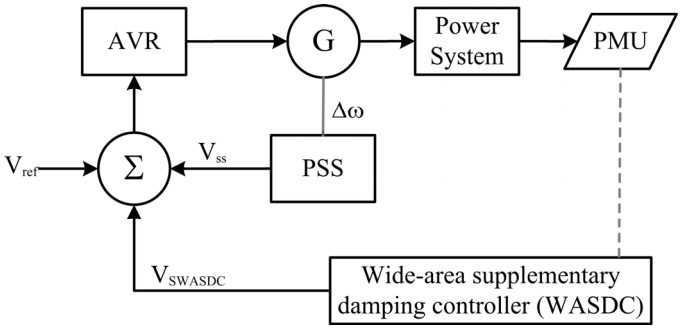

Fig. 2. General structure of wide-area damping control system

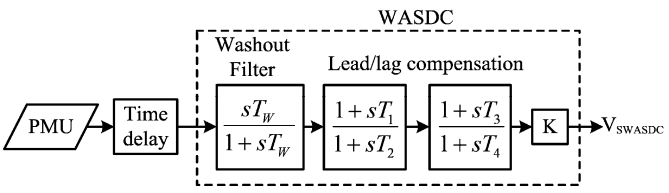

Fig. 3. Block diagram of the WASDC

Time delays are usually modeled by

$$G_{TD}(s) = e^{-T_d} \tag{15}$$

where T_d represents delay time.

For linear analysis purposes, the time delay can be modeled by Padé approximation. Thus, in this paper, the Padé second order approximation, which provides a good approximation for larger time delays [11], is used as given by

$$G_{appr}(s) = \frac{12 - 6T_d s + (T_d s)^2}{12 + 6T_d s + (T_d s)^2} \tag{16}$$

The parameters of the WASDC (i.e. proportional gain K and time constants T1 to T4), are determined by solving an optimization problem that accounts for small-stability requirements. The adopted formulation is derived from the method presented in [18] that pursues the minimization of the real part of critical eigenvalues as follows:

Minimize

$$\min FO = \sum_{i=1}^{nc} \alpha_i \tag{17}$$

subject to

$$\zeta_i \geq \zeta_{i\text{-min}} \tag{18}$$

$$|\Delta f_i| \geq \Delta f_{i\text{-min}} \tag{19}$$

$$\mathbf{x}_{j-min} \leq \mathbf{x}_j \leq \mathbf{x}_{j-max} \tag{20}$$

where α_i, ζ_i and Δf_i are the real part, the damping ratio and the frequency deviation of the i-th complex eigenvalue that constitutes a critical OM, $\mathbf{x}$ is the set of parameters of the WASDC (i.e. a solution of the optimization problem), and nc is the number of critical modes. Constraints (18) and (19) impose bounds on maximum tolerable mode frequency deviation and minimum acceptable mode damping ratio, respectively.

In this paper, a PSO algorithm, whose theoretical background is presented in [19], is employed, since it constitutes a powerful solver when applied to complex problems as demonstrated in several applications related to the power engineering field. Besides, a close to improved tuning of the WASDC is achieved by contemplating extreme operating states with maximum and minimum phase compensation requirements in order to account for a wide operating range.

IV. Test Results

Numerical experiments were performed on a HP Pavilion dv3 PC with Intel (R) Core (TM) 2 CPU, 2.2 GHz processing speed, and 4 GB RAM. The modeling, load flow, and modal analysis were accomplished by several routines written in Matlab which utilize some modified functions of the Power System Analysis Toolbox (PSAT) [20]. The QR method is used for full eigenvalue computation. The proposed approach is tested with a three area-seven machine benchmark power system (TASM) obtained by modifying the well known two area-four machine dynamic test system widely used for stability studies [8]. The single line diagram is depicted in Fig. 4. It basically consists of three similar areas connected through two long tie transmission lines. The tie transmission lines are relatively weak because of their distance of about 110 km.

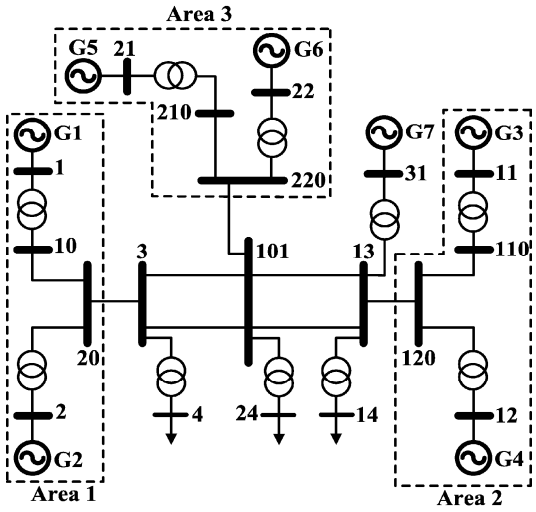

Fig. 4. Three area-seven machine power system

Each area has two thermal power plants. Conventional synchronous generators G1 to G6 are modeled using the subtransient model and equipped with fast static exciters and a simple thermal turbine-governor system whereas a single equivalent model was used to represent all individual units within the wind power plant G7 in order to avoid increasing computation time. Only generators G1 and G4 are equipped with PSSs. The single equivalent is represented using the dynamic model of the doubly-fed generator (DFG) described in [20]. This system exhibits five OMs: one inter-area mode, in which the generating units G1 and G2 oscillate against G3 and G4, a second inter-area mode in which G5 and G6 oscillate against the rest of the system, and three local modes, one in each area, associated with the oscillations of the generating units within each area. Uncertainty about nodal demands is modeled around highly load conditions based on Gaussian probabilistic models. G1 acts as the slack generator. The probabilistic models constructed for loads at buses 4, 14 and 24 are shown in Table I.

It is considered that the system has sufficient damping when the critical modes have $\zeta \geq 5\%$ for all operating conditions, including operating conditions following system element outages. The purpose of this criterion is to ensure that, in small-signal stability-secure operating conditions, no OM in the system has a damping ratio less than the specified threshold [14].

TABLE I
Probabilistic Distribution Functions of Nodal Active Power Demands

Bus	Mean (MW)	Standard deviation
4	973.97	16.649
14	1977.90	51.415
24	1149.20	22.376

A. Inter-area mode statistics and the impact of wind power

Overall CPU time for Monte Carlo-based Probabilistic eigenanalysis, without considering the wind power plant G7 (i.e. baseline case), with 1238 trials is 2.10 h. A set of five OMs was registered in all analyzed viable operating states. The parameters of these modes are in ascendent order according to their increasing mean frequency as shown in Table II. It can be seen that only the inter-area mode 1 (G1 and G2 vs. G3 and G4) has a mean damping ratio below 5% and hence it is considered as the main threat to system small-signal stability. By contrast, all the remaining OMs are not considered critical since and their damping ratio is greater than 5 % in all simulated operating states. Results for R_{Inst} index, which are given in Table III, further confirm that the instability of the system due to poorly damped inter-area mode 1 is highly probable.

TABLE II
BASELINE CASE: STATISTIC OF SYSTEM OSCILLATORY MODES

		Damping (%)		Frequency (Hz)	
Mode	**Gen. Units**	**Mean**	**Std**	**Mean**	**Std**
Inter-area 1	G1G2 vs. G3G4	3.7542	0.5986	0.6094	0.0153
Inter-area 2	G5G6 vs. G1G3	7.5642	0.1922	0.9004	0.0080
Local 1	G1 vs. G2	10.6197	0.5039	1.0656	0.0056
Local 2	G3 vs. G4	10.0390	0.2443	1.2334	0.0089
Local 3	G5 vs. G6	16.1761	0.0868	1.3621	0.0058

TABLE IIII
BASELINE CASE: R_{INST} INDEX

	R_{Inst}		
Mode	**$OM_{\zeta\text{-Neg}}$**	**$OM_{\zeta\text{-Poor}}$**	**$OM_{\zeta\text{-Damp}}$**
Inter-area 1	0.00	1.00	0.00
Inter-area 2	0.00	0.00	1.00
Local 1	0.00	0.00	1.00
Local 2	0.00	0.00	1.00
Local 3	0.00	0.00	1.00

The influence of wind power generation on the inter-area mode is analyzed by considering different incorporation levels of wind power penetration ranging from 100 MW to 400 MW. Results are summarized in Table IV. Note that the damping ratio of the inter-area mode 1 increases as the as the contribution from wind power plant G7 increases. This is reasonable since the introduction of wind generation led to considerable changes in network power flows resulting in lesser network congestion through tie lines between nodes 3 and 13, which is also highly desirable from the viewpoint of system small-signal stability performance. Besides, these results match with one of the conclusions established in [21]. Based on the R_{Inst} index, further analysis, as shown in Table V for the initial 100 MW penetration and the final 400 MW penetration levels, reveals that although wind power plant G7 has the potential to indirectly lead to slight increase in damping of inter-area mode 1 by altering the dispatch of synchronous generation and altering the power flows in the transmission network, more countermeasures are needed in order to fully eliminate the instability risk associated to this OM. In this connection, the next step is to design the WASDC.

B. Selection of the WASDC input and its location

Table VI shows the computed mean value of observability indexes for inter-area mode. For sake of brevity, only the three highest values are shown in the Table. It can be seen that, for this case study, the voltage angle of bus 120 exhibit good performances at any wind power integration level. Hence, the observability of inter-area mode 1 remains almost invariant at any level of wind generation.

TABLE IV
IMPACT OF WIND POWER GENERATION ON INTER-AREA MODE 1

		Damping (%)		Frequency (Hz)	
G7 active power (MW)	**G1 to G6 active power (MW)**	**Mean**	**Std**	**Mean**	**Std**
100 MW	4121.71	2.4903	0.5502	0.5954	0.0044
140 MW	4095.35	2.7721	0.5226	0.5963	0.0044
170 MW	4072.65	2.9473	0.5536	0.5970	0.0047
200 MW	4048.12	3.1233	0.5939	0.5980	0.0055
240 MW	4013.47	3.3497	0.6462	0.6005	0.0081
270 MW	3986.15	3.5063	0.6824	0.6037	0.0106
300 MW	3958.63	3.6341	0.7111	0.6081	0.0128
350 MW	3912.69	3.7702	0.7393	0.6160	0.0147
400 MW	3865.67	3.8268	0.7527	0.6227	0.0160

TABLE V
IMPACT OF WIND POWER GENERATION ON R_{INST} INDEX

		R_{Inst}		
	Mode	**$OM_{\zeta\text{-Neg}}$**	**$OM_{\zeta\text{-Poor}}$**	**$OM_{\zeta\text{-Damp}}$**
Initial	Inter-area 1	0.00	0.97	003
	Inter-area 2	0.00	0.00	1.00
	Local 1	0.00	0.00	1.00
	Local 2	0.00	0.00	1.00
Final	Inter-area 1	0.00	0.94	0.06
	Inter-area 2	0.00	0.00	1.00
	Local 1	0.00	0.00	1.00
	Local 2	0.00	0.00	1.00

TABLE III
IMPACT OF INCREASE OF WIND FARM GENERATION IN OBSERVABILITY INDEXES INTER-AREA MODE 1

	Mean Value of Observability Indexes (p.u.)		
Wind Generation	**Voltage Angle Bus 120**	**Voltage Angle Bus 14**	**Voltage Angle Bus 13**
100 MW	1.000	0.998	0.998
140 MW	1.000	0.998	0.998
170 MW	1.000	0.998	0.998
200 MW	1.000	0.997	0.997
240 MW	1.000	0.994	0.996
270 MW	0.999	0.997	0.992
300 MW	0.997	0.987	0.998
350 MW	0.991	0.975	0.980
400 MW	0.983	0.959	0.980

Subsequently, results shown in table VII provide the basis to choose the control location among the generators belonging to the power system. The highest controllability index is associated to generator G4. Therefore, this generating unit is considered as the best site to locate the WASDC in order to enhance the damping of inter-area mode 1. Moreover, note that the controllability does not change significantly as the penetration level of wind generation increases.

TABLE IVII
IMPACT OF INCREASE OF WIND FARM GENERATION IN CONTROLLABILITY INDEXES. INTER-AREA MODE 1

	Mean Value of Controllability Indexes (p.u.)		
Wind Generation	**Generator 4**	**Generator 3**	**Generator 1**
100 MW	0.991	0.999	0.774
140 MW	0.995	0.997	0.794
170 MW	0.998	0.994	0.814
200 MW	1.000	0.987	0.826
240 MW	1.000	0.981	0.836
270 MW	1.000	0.977	0.824
300 MW	1.000	0.976	0.808
350 MW	1.000	0.984	0.773
400 MW	1.000	0.991	0.727

C. WASDC implementation

The WASDC is located in generator 4. The voltage angle of bus 120 is chosen as the input signal of the controller. Also, time delay is fixed at 150 ms. Next, optimal tuning of the WASDC was performed by solving the optimization problem (17) – (20) through PSO. Probabilistic eigenanalysis is performed again considering the addition of the WASDC. Results are summarized in Table VIII to Table IX. From Table VIII, it can be seen that mean value of damping of the inter-area mode increases significantly from 3.75% to 29.30%. Also, note that the frequency of this mode is almost constant, which is important for supervision purposes. Table IX shows the evolution of the damping of the inter-area mode 1, considering the addition of the WASDC, as penetration level of wind power increases. Note that the damping ratio is above the threshold of 5% at all penetration levels. Further analysis based on the values of the R_{Inst} index also confirmed that all system OMs always exhibit a satisfactory damping throughout all viable operating states, which further support the effectiveness of the WASDC in enhancing the system small-signal stability performance.

V. CONCLUSIONS

In this paper, an approach to the design of a wide-area supplementary damping controller in order to improve the damping of inter-area oscillatory modes in wind-thermal power systems was presented. Probabilistic indexes of controllability and observability were developed based on probabilistic eigenanalysis and the concept of synthetic controllability and observability in order to determine suitable controller location as well as to perform proper selection of the input signal of the controller. The tuning of the controller through particle swarm optimization is realized while accounting for small-signal stability requirements. The impact of wind power on the small-signal stability performance was also investigated. It was found out that, for this case study, large wind power integration can have a positive impact on the damping of inter-area mode when increasing wind power generation helps in reducing the congestion through weak interconnections. Also, it was found out that the observability and controllability of the analyzed inter-area mode remain almost invariant independently of the wind power penetration level. The proposed approach should be further tested on larger realistic power systems to ascertain if the indicative findings of this work can be confirmed by a large scale case study since speaking in terms of energy penetration levels (that is the ratio of the wind energy delivered divided by the total energy delivered), the actual penetration levels in some pioneer countries, such as Germany, Spain and Denmark are above 8%, 6% and 20% respectively [22].

TABLE VII
ASSESSMENT OF DAMPING ENHANCEMENT USING THE WASDC INTER-AREA MODE 1

	Damping (%)		Frequency (Hz)	
	Mean	**Std.**	**Mean**	**Std**
Without WASDC	3.7542	0.5986	0.6094	0.0153
WASDC	29.3030	4.4553	0.5992	0.0105

TABLE IX
IMPACT OF WIND POWER GENERATION ON INTER-AREA MODE 1 SYSTEM WITH WASDC

		Damping (%)		Frequency (Hz)	
Wind Power Generation	**Conventional Generation (MW)**	**Mean**	**Std**	**Mean**	**Std**
100 MW	4112.49	33.7827	0.7068	0.5848	0.0029
140 MW	4095.35	33.5273	0.5760	0.5877	0.0013
170 MW	4039.23	33.3601	0.5730	0.5892	0.0010
200 MW	4021.69	33.0534	1.1345	0.5910	0.0024
240 MW	3979.38	32.1082	2.3577	0.5940	0.0048
270 MW	3943.28	30.9104	3.0729	0.5972	0.0061
300 MW	3914.32	29.5300	3.4956	0.6007	0.0067
350 MW	3856.84	26.5781	3.3297	0.6068	0.0058
400 MW	3806.26	24.2818	2.8451	0.6110	0.0056

REFERENCES

[1] S. Zhu, Y. Zhang, D. Le, and A. A. Chowdhury, "Understanding stability problems in actual system - Case studies," *IEEE Power and Energy Society General Meeting*, pp. 1-6, 2010.

[2] L. Grigsby, *Power system stability and control*, Boca Raton: Taylor & Francis Group, 2007.

[3] CIGRE Task Force 38.01.07,"Analysis and control of power system Oscillations," CIGRE Technical Brochure, Dec. 1996.

[4] M. R. Aghamohammadi, and A. Beik-Khormizi, "Small signal stability constrained rescheduling using sensitivities analysis by Neural Network as a preventive tool," *IEEE PES Transmission and Distribution Conference and Exposition*, pp. 1-5, 2010.

[5] Y. Li, and V. Venkatasubramanian, " Coordination of transmission path transfers," *IEEE Transactions on Power Systems*, vol. 19, no. 3, pp. 1607-1615, Ago. 2004.

[6] J. Condren, and T. W. Gedra, "Expected-security-cost optimal power flow with small-signal stability constraints," *IEEE Transactions on Power Systems*, vol. 21, no. 4, pp. 1736-1743., Nov. 2006.

[7] S.P. Teeuwsen, I. Erlich, and M.A. El-Sharkawi, "Methods for estimation of counter measures to improve oscillatory stability in power systems", *15th Power Systems Computation Conference*, Liege, Belgium, Aug. 2005.

[8] P. Kundur, *Power system stability and control*, New York: McGraw-Hill, 1994.

[9] A.F. Snyder, N. Hadjsaid, D. Georges, L. Mili, A.G. Phadke, O. Faucon, and S. Vitet, "Inter-area oscillation damping with power system stabilizers and synchronized phasor measurements," *International Conference on Power System Technology*, vol. 2, pp. 790-794, 1998.

[10] X. Xie, J. Xiao, C. Lu, and Y. Han, "Wide-area stability control for damping inter-area oscillations of interconnected power systems," *IEE Proceedings - Generation, Transmission and Distribution*, vol. 153, no. 5, pp. 507-514, 2006.

[11] A. G. Phadke, and J. Thorp, *Synchronized Phasor Measurements and Their Applications*, New York: Springer, 2008.

[12] C. Martinez, J. Parashar, J. Dyer, and J. Coroas, "Phasor Data Requirements for real time Wide-Area Monitoring, Control and Protection Applications," CERTS/EPG, Jan. 2005.

[13] J. F. Hauer, D. J. Trudnowski, and J. G. DeSteese, "A Perspective on WAMS Analysis Tools for Tracking of Oscillatory Dynamics," *IEEE Power Engineering Society General Meeting*, pp. 1-10, 2007.

[14] J. L. Rueda, D. G. Colomé, and I. Erlich, "Assessment and enhancement of small signal stability considering uncertainties", *IEEE Transactions on Power Systems*, Vol. 24, No. 1, pp. 198-207, Feb. 2009.

[15] Y. Zhang, and A. Bose, "Design of Wide-Area Damping Controllers for Inter-area Oscillations," *IEEE Transactions on Power Systems*, vol. 23, no. 3, pp. 1136-1143, 2008.

[16] D. K. Lindner, J. Babendreier, and A. A. Hamdan, "Measures of controllability and observability and residues," *IEEE Transactions on Automat Control*, vol. 34, no. 6, pp. 648–50, 1989.

[17] A. Heniche, and I. Kamwa, "Assessment of Two Methods to Select Wide-Area Signals for Power System Damping Control," *IEEE Transactions on Power Systems*, vol. 23, no. 2, pp. 572-581, 2008.

[18] A. Mendonça, and J. Peças Lopes, "Robust tuning of PSS in power systems with different operating conditions," *IEEE Bologna Power Tech Conference Proceedings*, vol. 1, 2003.

[19] J. Kennedy, R. C. Eberhart, and Y. H. Shi, *Swarm Intelligence*, Academic Press, 2001.

[20] F. Milano, L. Vanfretti, and J.C. Morataya, "An Open Source Power System Virtual Laboratory: The PSAT Case and Experience," *IEEE Transactions on Education*, vol. 51, no. 1, pp 17 - 23, Feb. 2008.

[21] J. L. Rueda, and F. Shewarega, "Small signal stability of power systems with large scale wind power integration", *Proceedings of the CIGRE XIII ERIAC - Iberian-American Regional Meeting*, Puerto de Iguazú, Argentina, May 2009.

[22] J. C. Smith, and B. Parsons, "What does 20% look like?," *IEEE Power and Energy Magazine*, Vol. 5, No. 6, Nov.-Dec. 2007, pp. 22-33.

Carlos A. Juárez (GS'07) was born in 1983. He obtained the Electrical Engineer degree from Universidad Centroamericana José Simeón Cañas in 2005. He has worked in the Electronic and Informatics Department of that same University during 2005 and 2006. Since 2007, he has been pursuing his Ph.D. degree in Electrical Engineering in the Instituto de Energía Eléctrica (IEE), at the Universidad Nacional de San Juan, Argentina as a part of a four-year scholarship financed through the German Academic Exchange Service (DAAD, by the acronym in German) Regional Program. His main fields of interest are control and supervision of power systems, power system stability and signal processing.

José L. Rueda (M'10) was born in 1980. He received the Electrical Engineer diploma from the Escuela Politécnica Nacional (EPN), Quito, Ecuador, in 2004, and the Ph.D. degree in electrical engineering from the Universidad Nacional de San Juan, San Juan, Argentina, in 2009. From September 2003 till February 2005, he worked in Ecuador, in the fields of industrial control systems and electrical distribution networks operation and planning. Currently, he is pursuing postdoctoral research at the Institute of Electrical Power Systems (EAN, by the acronym in German), as a part of a one-year scholarship financed by the University Duisburg-Essen. His current research interests include power system stability and control, system identification, power system planning, probabilistic and artificial intelligent methods, and wind power.

István Erlich (SM'08) was born in 1953. He received the Dipl.-Ing. degree in electrical engineering and the Ph.D. degree from the University of Dresden, Dresden, Germany, in 1976 and 1983, respectively. After his studies, he worked in Hungary in the field of electrical distribution networks. From 1979 to 1991, he was with the Department of Electrical Power Systems of the University of Dresden. In the period of 1991 to 1998, he worked with the consulting company EAB, Berlin, Germany, and the Fraunhofer Institute IITB Dresden, respectively. During this time, he also had a teaching assignment at the University of Dresden. Since 1998, he has been a Professor and head of the Institute of Electrical Power Systems at the University of Duisburg-Essen, Duisburg. Germany. His major scientific interest is focused on power system stability and control, modelling, and simulation of power system dynamics, including intelligent system applications. Dr. Erlich is a member of VDE and the chairman of the IFAC (International Federation of Automatic Control) Technical Committee on Power Plants and Power Systems.

Delia G. Colomé was born in 1959. She obtained the Electrical Engineer degree and the Ph.D. degree in Electrical Engineering from Universidad Nacional de San Juan, in 1985 and 2009, respectively. Since 1983, she has been a researcher at Instituto de Energía Eléctrica, Universidad Nacional de San Juan, Argentina. During this time, she has worked as project manager in numerous technical support projects in Argentina and different Latin-American countries. Currently, she is a Professor in the Undergraduate and Postgraduate programs at Instituto de Energía Eléctrica. Her main fields are control an supervision of power systems, modeling and simulation of power systems, and the development of computational tools for engineering teaching..